

# A Triplet Based Approach for Indexing of Fingerprint Database for Identification

Bir Bhanu and Xuejun Tan  
Center for Research in Intelligent Systems  
University of California, Riverside, CA92521, USA  
Email: {bhanu, xtan}@cris.ucr.edu

**Abstract.** This paper presents a model-based approach which efficiently retrieves correct hypotheses using properties of triangles formed by the triplets of minutiae as the basic representation unit. We show that the uncertainty of minutiae locations associated with feature extraction and shear does not affect the angles of a triangle arbitrarily. Geometric constraints based on characteristics of minutiae are used to eliminate erroneous correspondences. We present an analysis to characterize the discriminating power of our indexing approach. Experimental results on fingerprint images of varying quality show that our approach efficiently narrows down the number of candidate hypotheses in the presence of translation, rotation, scale, shear, occlusion and clutter.

## 1 Introduction

Fingerprints have long been used for personal recognition. There are two kinds of fingerprint based biometric systems in terms of their utilization: verification and identification. In verification, the input includes a fingerprint image and an ID, the system then verifies whether the image is consistent with the ID. In identification, the input is only a fingerprint image and the system identifies fingerprint images in the database corresponding to the input fingerprint image. The problem of identifying a fingerprint image can be stated as: given a fingerprint database and a test fingerprint image, in the presence of translation, rotation, scale, shear, occlusion and clutter, does the test image resemble any of the fingerprints in the database? It is still a challenging problem. Recent techniques of fingerprint recognition are presented in [1]-[3]. All of them are for verification. Like our approach, Germain et al. [4] use the triplets of minutiae in the indexing procedure. However, the features they use are different from ours. The features they use are: the length of each side, the ridge counts between each pair, and the angles measured with respect to the fiducial side. The problems with their algorithm are: (a) the length changes are not insignificant under scale and shear; (b) the ridge count and the angle are both very sensitive to the quality of images. As a result, they have to use large size of bins to tolerate distortions, which reduces the size of index space and degrades the performance of their algorithm greatly. The key contributions of our work are to present a new indexing algorithm based on features derived from the triplets of minutiae and to demonstrate the power of it on a fingerprint database of 1000 images.

## 2 Triplet-based Features for Indexing

The triangle features that we use are its angles, orientation, type, direction and maximum side.

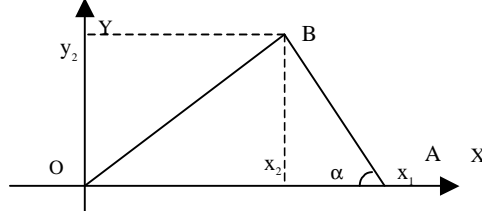


Fig. 1. Illustration of variables.

**2.1 Analysis of Angle Changes under Distortions:** It can be proved that angles are invariant under translation, rotation and scale. However, the transform between the different impressions of the same finger also includes the uncertainty of minutiae locations, which is associated with feature extraction and shear. Thus, the location of each minutia translates in a small local area randomly and independently.

Fig. 1 shows a triangle. Without loss of generality, we assume one vertex, O, of the triangle is (0, 0), and it does not change under distortions. Suppose the positions of points A and B are  $(x_1, 0)$  and  $(x_2, y_2)$ ,  $x_1 > 0$ ,  $y_2 > 0$  and  $x_2 \in (-\infty, +\infty)$ . Because of the uncertainty of locations, A and B move to  $(x_1 + \Delta x_1, 0)$  and  $(x_2 + \Delta x_2, y_2 + \Delta y_2)$ , and  $\alpha$  changes to  $\alpha + \Delta\alpha$ , respectively. Since for small  $\Delta\alpha$ ,  $\tan\Delta\alpha \approx \Delta\alpha$ , we have

$$\Delta\alpha \approx \tan\Delta\alpha = \frac{(x_1 - x_2)\Delta y_2 - y_2(\Delta x_1 - \Delta x_2)}{(x_1 - x_2)^2 + (x_1 - x_2)(\Delta x_1 - \Delta x_2) + y_2^2 + y_2\Delta y_2} \quad (1)$$

We want to compute the expectation of  $|\Delta\alpha|$ . Suppose  $\Delta x_1$ ,  $\Delta x_2$ , and  $\Delta y_2$  are independent, and  $-4 \leq \Delta x_i, \Delta y_2 \leq 4$ ,  $i = 1, 2$ , and  $\Delta x_i$  and  $\Delta y_2$  are all integers, then

$$g(x_1, x_2, y_2) = E\{\Delta\alpha\} \approx \sum_{\Delta x_1=-4}^4 \sum_{\Delta x_2=-4}^4 \sum_{\Delta y_2=-4}^4 ( |\tan\Delta\alpha| \times p(\Delta x_1) p(\Delta x_2) p(\Delta y_2) ) \quad (2)$$

Suppose  $p(\Delta x_1)$ ,  $p(\Delta x_2)$  and  $p(\Delta y_2)$  are discrete uniform distributions in  $[-4, +4]$ . Let  $0 < x_1, y_2, |x_2| < L$ , where  $L$  is the maximum value of these variables in the image (in our experiments,  $L = 150$ ). We compute  $g(x_1, x_2, y_2)$  at each point  $(x_1, x_2, y_2)$  based on whether  $\alpha$  is the minimum, median or maximum angle in the triangle.

From Table 1, we observe: (a) the percentages of the expectation of changes of angles less than the threshold for minimum angle and median angle are always greater than that for the maximum angle; (b)  $2^\circ$  is a good threshold for dealing with changes caused by minutiae locations uncertainty in  $[-4, +4]$ . The percentages of the expectation of changes of angles less than  $2^\circ$  are 93.2% and 87.3% for  $\alpha_{\min}$  and  $\alpha_{\text{med}}$ , respectively. Using other distributions for  $p(\Delta x_1)$ ,  $p(\Delta x_2)$  and  $p(\Delta y_2)$ , we find the results similar to that in Table 1.

**Table 1.** Percentage of the expectation of changes of angles less than the threshold.

Angle's Type	Angle Change Threshold					
	1°	2°	3°	4°	5°	6°
$\alpha_{\min}$	51.6	93.2	98.5	99.6	99.9	100.0
$\alpha_{\text{med}}$	56.6	87.3	94.5	97.3	98.7	99.4
$\alpha_{\max}$	1.0	67.7	87.3	94.2	97.2	98.7

## 2.2 Index Elements and Geometric Constraints:

**2.2.1 Indexing Function:** Index elements are the features that are used to construct the indexing function  $H(\alpha_{\min}, \alpha_{\text{med}}, \phi, \gamma, \eta, \lambda)$ . Note that only the hypotheses extracted within the tolerance used for the parameters in the indexing function  $H$  are passed on for checking the geometric constraints.

- **Angles  $\alpha_{\min}$  and  $\alpha_{\text{med}}$ :** Suppose  $\alpha_i$  are three angles in the triangle,  $i = 1, 2, 3$ . Let  $\alpha_{\max} = \max\{\alpha_i\}$ ,  $\alpha_{\min} = \min\{\alpha_i\}$ ,  $\alpha_{\text{med}} = 180^\circ - \alpha_{\max} - \alpha_{\min}$ , then the label of the triplets in this triangle is such that if the minutia is the vertex of angle  $\alpha_{\max}$ , we label this point as  $P_1$ ; if the minutia is the vertex of angle  $\alpha_{\min}$ , we label it as  $P_2$ ; the last minutia is labeled as  $P_3$ . We use  $\alpha_{\min}$  and  $\alpha_{\text{med}}$  as two elements in the indexing function  $H$ .  $0^\circ < \alpha_{\min} \leq 60^\circ$  and  $\alpha_{\min} \leq \alpha_{\text{med}} < 90^\circ$ .

- **Triangle Orientation  $\phi$ :** Let  $Z_i = x_i + jy_i$  be the complex number ( $j = \sqrt{-1}$ ) corresponding to the coordinates  $(x_i, y_i)$  of point  $P_i$ ,  $i = 1, 2, 3$ . Define  $Z_{21} = Z_2 - Z_1$ ,  $Z_{32} = Z_3 - Z_2$ , and  $Z_{13} = Z_1 - Z_3$ . Let  $\phi = \text{sign}(Z_{21} \times Z_{32})$ , where  $\text{sign}$  is the signum function and  $\times$  is the cross product of two complex numbers.  $\phi = 1$  or  $-1$ .

- **Triangle Type  $\gamma$ :** Let  $\gamma = 4\gamma_1 + 2\gamma_2 + \gamma_3$ , where  $\gamma_i$  is the feature type of point  $P_i$ ,  $i = 1, 2, 3$ . If point  $P_i$  is an end point, then  $\gamma_i = 1$ , else  $\gamma_i = 0$ ,  $0 \leq \gamma \leq 7$ .

- **Triangle Direction  $\eta$ :** Search the minutia from top to bottom and left to right in the image, if the minutia is the start point of a ridge or valley, then  $v = 1$ , else  $v = 0$ . Let  $\eta = 4v_1 + 2v_2 + v_3$ ,  $v_i$  is the  $v$  value of point  $P_i$ ,  $i = 1, 2, 3$ .  $0 \leq \eta \leq 7$ .

- **Maximum Side  $\lambda$ :** Let  $\lambda = \max\{L_i\}$ , where  $L_1 = |Z_{21}|$ ,  $L_2 = |Z_{32}|$ , and  $L_3 = |Z_{13}|$ .

**2.2.2 Geometric constraints:** These are used to eliminate any erroneous correspondences obtained from the above step.  $\delta_1$ ,  $\delta_2$  and  $\delta_3$  tolerate rotation and errors in estimating the local orientation and  $\delta_4$  tolerates translation.

- Let points  $P_{21}$ ,  $P_{32}$ , and  $P_{13}$  be the midpoint of line  $P_2P_1$ ,  $P_3P_2$  and  $P_1P_3$ , respectively, and point  $P_{123}$  be the centroid of the triangle  $\Delta P_1P_2P_3$ . Let  $\phi_{21} = \psi_{21} - \psi_{123}$ ,  $\phi_{32} = \psi_{32} - \psi_{123}$ , and  $\phi_{13} = \psi_{13} - \psi_{123}$ , where  $\psi_{21}$ ,  $\psi_{32}$ ,  $\psi_{13}$  and  $\psi_{123}$  are the local orientation of points  $P_{21}$ ,  $P_{32}$ ,  $P_{13}$  and  $P_{123}$ , respectively. We have  $|\phi - \phi'| < \delta_1$ , where  $\phi$  and  $\phi'$  are  $\phi_{21}$ ,  $\phi_{32}$  or  $\phi_{13}$  in two impressions.

- Let  $\psi_i$  be the local orientation of point  $P_i$ , and  $\omega_i = \psi_i - \psi_{123}$ , we have  $|\omega - \omega'| < \delta_2$ , where  $i = 1, 2, 3$ ,  $\omega$  and  $\omega'$  are  $\omega_1$ ,  $\omega_2$  or  $\omega_3$  in two different impressions.

- Let  $\theta_{21} = \text{angle}(Z_{21})$ ,  $\theta_{32} = \text{angle}(Z_{32})$ , and  $\theta_{13} = \text{angle}(Z_{13})$ , where  $\text{angle}(Z)$  is the phase angle of the complex number  $Z$ . We have  $|\theta - \theta'| < \delta_3$ , where  $\theta$  and  $\theta'$  are  $\theta_{21}$ ,  $\theta_{32}$  or  $\theta_{13}$  of two different impressions.

- Let  $Z_c = (Z_1 + Z_2 + Z_3) / 3$ , we have  $|Z - Z'| < \delta_4$ , where  $Z$  and  $Z'$  are the  $Z_c$  in two different impressions.

The index score is computed according to the number of correspondences of triangles between the input image and images in the database.

### 2.3 Analysis of the Proposed Approach:

**2.3.1 Index Space and Discrimination:** Since there is uncertainty associated with minutiae locations, a binning mechanism must be used. We use  $0.5^\circ$  as the bin size for angle  $\alpha_{\min}$  and  $\alpha_{\text{med}}$ , and 10 pixels for the  $\lambda$ . The bin size allows an appropriate tolerance for different distortions where  $\alpha_{\min}$  and  $\alpha_{\text{med}}$  tolerate shear and  $\lambda$  tolerates scale. According to the range of features, the number of entries for the index space H is  $120 \times 180 \times 2 \times 8 \times 8 \times 20 = 55,296,000$  ( assume  $\lambda \leq 200$ , there are 20 bins for  $\lambda$  ). If there are 40 features in a image, then we have  ${}^{40}C_3 = 40 \times 39 \times 38 / 6 = 9,880$  triangles in the image. However, if  $\alpha_{\min} < \delta_\alpha$  or  $\tau < \delta_\tau$ , then the uncertainty of minutiae locations may have more effect on  $\alpha_{\min}$  and  $\alpha_{\text{med}}$ , so we do not use these triangles in the model-base, where  $\tau$  is the minimum length of the sides in a triangle. Thus, only about 1/3 of the triangles are taken as models (for  $\delta_\alpha = 10^\circ$ ,  $\delta_\tau = 20$ ). Suppose these triangles are uniformly distributed in the index space, then this approach can host  $55,296,000 / (9880/3) \approx 16790$  images with only one index in each entry. If there are N indices in each entry, then it can host  $16790 \times N$  images.

**2.3.2 Probability of False Indexing:** Suppose (a) S is the size of the index space; (b)  $f_k$  is the number of triangles in the model-base for image  $I_k$ , and these triangles are uniformly distributed in the index space; (c) b is the search redundancy for each triangle in the test image; (d)  $v_k$  is the number of corresponding triangles between image I and  $I_k$ ; (e)  $f_t$  is the number of triangles for the test image; (f)  $p_0$  is the probability to find a corresponding triangle in the index space for image  $I_k$  in a single search and  $p_1$  is the probability in redundant search, then

$$p_0 = \frac{f_k}{S} \quad \text{and} \quad p_1 = 1 - (1 - p_0)^b \quad (3)$$

Hence, we can estimate  $P\{v_k > T\}$  by the Poisson distribution with  $\xi = f_t \times p_1$ :

$$P\{v_k > T\} \approx 1 - e^{-\xi} \sum_{i=0}^T \frac{\xi^i}{i!} \quad (4)$$

When  $T = 25$ ,  $P\{v_k > T\} = 0.01$ . So,  $T = 25$  can be used as the threshold to reject a test image which has no corresponding image in the database. The triangles are not uniformly distributed in the model-base, however, we apply geometric constraints to eliminate erroneous correspondences, the value of T can be less than 25.

## 3 Experimental Results

**3.1 Database:** The data set used in our experiments has 1000 images. It includes 400 pairs of images and 200 single images. These images are collected under real-world conditions by a fingerprint optical sensor with the resolution of 300 DPI. The size of these images is  $248 \times 120$  pixels. Each pair of images are different impressions of the same finger, one is used to construct the model-base, and the other is used to test the indexing performance. The range of the distortions between each pair of images are: translation ( $\pm 30$  pixels), rotation ( $\pm 30^\circ$ ), scale ( $1 \pm 0.1$ ), and shear ( $\pm 4$  pixels). The single image data set is used to test the rejection performance. We subjectively classify the images according to their quality into three classes: good, fair and poor.

The quality of images is determined visually based on the criteria, such as distortions between images, contrast, ridges' continuity and width. A pair of images from each class is shown in Fig. 2.  $G_1$  is the image in the database and  $G_2$  is the test image. Notice the rotation between  $G_1$  and  $G_2$  in Fig. 2.1 and Fig. 2.2 and the dryness of the fingerprint reflected in the images in Fig. 2.3. Table 2 shows the composition of the database. Notice that most images in the database are of fair quality (33.2%) or poor quality (47.8%).

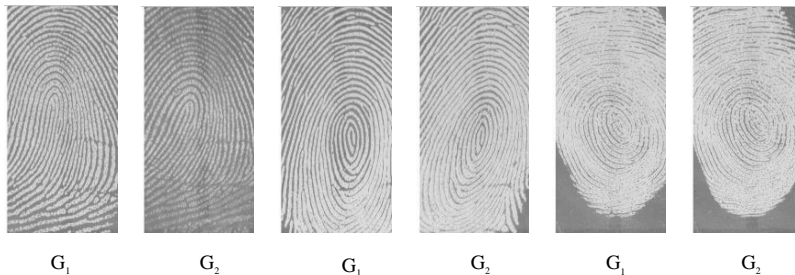


Fig. 2.1. Good images.

Fig. 2.2. Fair images.

Fig. 2.3. Poor images.

Table 2. Composition of the database.

	Images' Quality			Summary
	Good	Fair	Poor	
# of Pairs of Images	78x2	124x2	198x2	400x2
# of Single Images	34	84	82	200
% in DB	19.0	33.2	47.8	100.0

**3.2 Performance Evaluation Measures:** A test image, which has a corresponding image in the database, is said to be correctly indexed if it has enough corresponding triangles in the model-base and the correct corresponding image appears in a shortlist of hypotheses obtained by the indexing approach. The Correct Index Power (CIP) is defined as the ratio of the number of correctly indexed images to the number of images used to construct the model-base. A test image, which has no corresponding image in the database, is said to be correctly rejected if it does not have enough corresponding triangles in the model-base. The Correct Reject Power (CRP) is defined as the ratio of the number of correctly rejected images to the number of the test images that do not have corresponding images in the database.

**3.3 Experimental Results:** The parameters of the algorithm are:  $\delta_1 = \delta_2 = \delta_3 = 30^\circ$ ,  $\delta_4 = 50$ ,  $\alpha_1 = \alpha_2 = 2^\circ$ , and  $T = 20$ . The bin size of  $\lambda$  is 10. Minutiae are automatically extracted using a technique in [5].

Table 3 shows that images of different quality have different results using the proposed approach. The CIP of a single hypothesis for good quality image is 96.2%. As the quality of images becomes worse, the CIP decreases to 85.5% for fair and 83.3% for poor images. The CIP of a single hypothesis for the entire database is 86.5%. The most important result of our experiments is that the CIP for the top two hypotheses is 100% for good images, and for fair images and poor images, the CIP for the top five hypotheses are 99.2% and 98%, respectively. For the entire database, the CIP for the

top nine hypotheses is 100%. Further, all the 200 single images are rejected by our approach, thus, CRP is 100%. On a ULTRA2 workstation, average time for correctly indexing or correctly rejecting a test case is less than 1 second. It is much less than that of repeating a verification process (1 second [3]) for each image in the database.

**Table 3.** Correct Indexing Power of experimental results.

Top N Hypotheses	Image Quality			Sum. of the entire DB	
	Good	Fair	Poor		
N	1	96.2	85.5	83.3	86.5
	2	100	92.7	92.9	94.3
	3	100	95.2	95.5	96.3
	4	100	97.6	97.5	98.0
	5	100	99.2	98.0	98.8
	6	100	99.2	98.5	99.0
	7	100	99.2	100	99.8
	8	100	99.2	100	99.8
	9	100	100	100	100

## 5 Conclusions

Our experimental results show that the proposed indexing approach can greatly reduce the number of candidate hypotheses. The CIP of the top five and the top nine hypotheses are 98.8% and 100.0% for the entire database, respectively. This provides a reduction by a factor of more than 40 for the number of hypotheses that need to be considered for detailed matching. The CRP is 100.0%. Both CIP and CRP together characterize the discriminating power of our indexing approach. Our approach based on triplets of minutiae is promising for identifying fingerprints under translation, rotation, scale, shear, occlusion and clutter.

**Acknowledgments:** This work is supported in part by a grant from Sony, DiMI and I/O software. The contents and information do not necessarily reflect the positions or policies of the sponsors.

## References

1. R. Cappelli, A. Lumini, D. Maio, D. Maltoni, Fingerprint classification by directional image partitioning, *IEEE Trans. on PAMI*, Vol. 21, No. 5, pp.402-421, May 1999.
2. A.K. Jain, L. Hong, S. Pankanti and R. Bolle, An identity-authentication system using fingerprints, *Proc. of the IEEE*, Vol. 85, No. 9, pp.1364-1388, September 1997.
3. N.K. Ratha, K. Karu, S. Chen, and A.K. Jain, A real-time matching system for large fingerprint databases, *IEEE Trans. on PAMI*, Vol. 18, No. 8, pp.799-813, August 1996.
4. R.S. Germain, A. Califano, and S. Colville, Fingerprint matching using transformation parameter clustering, *IEEE Computational Science and Engineering*, Vol. 4, No. 4, pp.42-49, October/November 1997.
5. B. Bhanu, M. Boshra and X. Tan, Logical templates for feature extraction in fingerprint images, *Proc. Int. Conf. on Pattern Recognition*, Vol. 2, pp.850-854, September, 2000.